arXiv:0907.4623v1 [cond-mat.stat-mech] 27 Jul 2009

Energy Transport in an Ising Disordered Model

E. Agliari[1], M. Casartelli[1,2] and A. Vezzani[1,3]

[1] Dipartimento di Fisica, Università di Parma, Viale G.P. Usberti n.7/A (Parco Area delle Scienze) 43100 - Parma - ITALY

[2] INFN, gruppo collegato di Parma, Viale G.P. Usberti n.7/A (Parco Area delle Scienze) 43100 - Parma - ITALY

[3] CNR-INFM, National Research Center S3, via Campi 213/a, 41100 - Modena-ITALY

Abstract. We introduce a new microcanonical dynamics for a large class of Ising systems isolated or maintained out of equilibrium by contact with thermostats at different temperatures. Such a dynamics is very general and can be used in a wide range of situations, including disordered and topologically inhomogenous systems. Focusing on the two-dimensional ferromagnetic case, we show that the equilibrium temperature is naturally defined, and it can be consistently extended as a local temperature when far from equilibrium. This holds for homogeneous as well as for disordered systems. In particular, we will consider a system characterized by ferromagnetic random couplings $J_{ij} \in [1-\epsilon, 1+\epsilon]$. We show that the dynamics relaxes to steady states, and that heat transport can be described on the average by means of a Fourier equation. The presence of disorder reduces the conductivity, the effect being especially appreciable for low temperatures. We finally discuss a possible singular behaviour arising for small disorder, i.e. in the limit $\epsilon \to 0$.
keywords: Transport processes (Theory), Heat conduction, Disordered systems (Theory)

1. Introduction

Microcanonical dynamics seems to be a proper mode to describe an isolated system, or its isolated bulk, without any assumption on the equilibrium state between the system and the surrounding. A typical context where such a dynamics occurs is in the study of transport properties in continuous or discrete models (see [1] for general references). For instance, for a system in thermal contact with two heat reservoirs at different temperatures, energy may be exchanged only through the thermostats, and the internal dynamics requires an energy preserving evolution to be implemented in the microcanonical framework; analogous considerations hold for matter transport and similar items [2, 3, 4].

Presently, we are interested in heat transport in discrete models, namely spin systems. As it is well known, for such systems there exist several rules to simulate microcanonical evolution, e.g. the Q2R rule introduced by Vichniac, the Creutz rule and, more recently, the KQ rule [5, 6, 7, 8, 9]. All of them present some weak aspects which require the introduction of some constraints concerning geometrical support, boundary conditions (i.e. the allowed range of imposed temperatures), connectivity, homogeneity, etc. Our purpose is to introduce a microcanonical dynamics sufficiently flexible to be adapted to all these cases. The recent interest in systems displaying

quenched disorder and inhomogeneous structure, provides indeed a strong motivation for the development of such a general dynamics [10, 11, 12, 13, 14].

As it is well known, Q2R and Creutz dynamics differ in the fact that the latter supplies each site in the lattice with a possible bounded reserve of "kinetic" energy, in such a way that the spin flip is allowed not only when the magnetic energy is preserved (as in Q2R), but also when the energy excess or defect may be assigned to or extracted from the reserve, so that the *total* energy is preserved. This additional possibility, however, does not solve the dynamical freezing at low energy densities (occurring of course also in Q2R), since in such conditions one easily falls into short periodical cycles, inhibiting the transport of heat and the exploration of the whole set of configurations at constant energy. In other terms, both Creutz and Q2R dynamics have an ergodicity breakdown at low energy, loosing the independence of initial conditions which is necessary to ensure a statistical effectiveness to the dynamical description. Moreover, one should introduce *ad hoc* modifications when the connectivity is not homogeneous. As to the KQ dynamics, introduced and discussed in [8, 9], even if it possesses the wanted ergodicity, it is not a satisfying solution to the general dynamical problem, since it is specifically meant for regular lattices.

The new dynamics we are going to define actually modifies the Creutz scheme, only maintaining the distinction between magnetic and kinetic energies. As we shall see, not only it displays effective ergodicity for all practical purposes, but it can also be easily adapted to a wide class of spin systems without any substantial modification, exhibiting therefore the desired versatility. In particular, it can be implemented on arbitrary topologies, even non regular ones. Another aspect of this flexibility is that the extension to inhomogeneous systems, where the spin coupling is not a constant, is quite natural. Hence, a great variety of disordered models become easily accessible in principle; in the following we study an example of quenched disorder.

It is worth underlining that, in all the cases considered here, the magnetic and kinetic energies result to be non correlated: this allows a natural definition of temperature at equilibrium, which, in a very natural way, depends only on the average kinetic energy. This approach can be consistently extended, when far from equilibrium, to a definition of *local* temperature. Now, dealing with heat transport, this implies an important improvement in the description of steady states, since not only diffusivity but also conductivity become easily computable. In particular, in studying a model of quenched disorder, the interesting point is to explore how inhomogeneity affects the thermal and transport properties. For instance, we verify that the conductivity becomes smaller as the disorder grows. The emergence of non analytical behaviour in the limit of vanishing disorder is also observed.

In the following, we first describe in details how our microcanonical dynamics works (Section 2) and we show that it is able to relax the system to well defined steady states (Section 3), even in the presence of disorder (Section 4), verifying that a temperature as an intensive quantity independent of the actual values of couplings can still be defined. Then, we focus on the transport properties (Section 5), and on the effect of disorder on the conductivity (Section 6). The last section is devoted to our conclusions and final remarks (Section 7).

2. Microcanonical Dynamics

Let us consider an Ising model defined on a generic network. In particular, $s_i = \pm 1$ denotes the i-site spin; on each link $i \sim j$ we introduce a local exchange interaction

J_{ij}, so that the magnetic energy of a link is $J_{ij}s_is_j$. Moreover, on the link $i \sim j$ we define a local *kinetic energy* $E_{ij} > 0$. We remark that while standard Creutz scheme specifies a bounded amount of "kinetic" energy in each site, we introduce an energy defined on links which is non-negative but, in principle, unbounded. The dynamical rule proceeds as follows:

(i) Start from a distribution of energies E_{ij};

(ii) choose randomly a link $i \sim j$;

(iii) extract one over the possible four spin-configurations for the couple of sites i, j, and evaluate the magnetic energy variation ΔE^m induced by the move, where ΔE^m allows for energy variations occurred on the link $i \sim j$ as well as on those pertaining to links adjacent to sites i or j;

(iv) if $\Delta E^m \leq 0$ accept the move and increase the link energy E_{ij} of ΔE^m. When $\Delta E^m > 0$, accept the move and decrease the link energy of ΔE^m only if $E_{ij} \geq \Delta E^m$.

Three main points have to be remarked:

- Every link is defined by its extremes not only in rectangular lattices but in all graphs, even in the case of variable connectivity. This ensures a great flexibility with respect to the underlying geometry.
- The interchange between sites and links allows the energy to travel throughout the graph, even at low energy density, without the freezing of the standard Creutz-Q2R rules or the geometrical restrictions of the KQ dynamics.
- The constraint of uniform couplings $J_{ij} \equiv J = const$, typical of previous microcanonical dynamics, can also be relaxed as our dynamics allows to use local (i.e. non uniform) spin interactions.

Clearly, the above dynamics conserves the total energy given by the following *Hamiltonian* function

$$H(s_i, E_{ij}) = \sum_{i \sim j} \left(J_{ij} s_i s_j + E_{ij} \right), \tag{1}$$

where the sum runs over all the links of the network. Notice that energy is locally conserved, namely long-range energy transfers are forbidden and hence we can define our dynamics as microcanonical, where the kinetic energy energy E_{ij} works as an additional degree of freedom. Expression (1) is very general, representing a conserved energy for a model defined on a generic network. Moreover, according to the choice of the couplings J_{ij}, a wide class of models (disordered interactions, vacancies, spin glasses etc.) can be recovered.

Actually, for comparisons and checks, we consider first the homogeneous system $J_{ij} \equiv J$ (with $J \equiv 1$ in simulations) on the standard rectangular lattice of L_X columns and L_Y rows, both in the toroidal geometry (periodical boundaries) and in the cylindrical geometry with two opposite boundaries. Such boundaries can be "free" (i.e. three neighbours for each site) or "open" (i.e. in contact with a reservoir). Heat conduction in the latter case was studied e.g. in [15, 16] using Q2R-Creutz dynamics, in [8, 9] using KQ dynamics and in [17] using a layer heat-bath.

Afterward, we shall study the transport properties in a cylindrical system where the couplings $\{J_{ij}\}$ are chosen randomly in the interval $[1-\epsilon, 1+\epsilon]$, i.e. a disordered ferromagnet.

3. Temperature and Dynamical checks

At equilibrium, i.e. in a closed system where no energy is injected or subtracted, every move is reversible, and the probability $P(S \to S')$ to go from the configuration S to the configuration S' equals $P(S' \to S)$. Detailed balance is satisfied, and the equilibrium probability distribution is constant over all configurations.

If all the configurations with the same energy are visited in the evolution, the system is ergodic and its equilibrium properties can also be described by Boltzmann statistics. In this perspective, we check the agreement between the numerical stationary results and the Boltzmann distribution, focusing first on the homogeneous system $J_{ij} \equiv J$ defined on a two-dimensional torus; a positive response to the check has to be seen as an indication of effective ergodicity.

A first step in this direction consists in testing the decorrelation between the kinetic energy E_{ij} and the magnetic energy Js_is_j of a link. Indeed, we verify that for each link

$$\langle E_{ij} J s_i s_j \rangle = \langle E_{ij} \rangle \langle J s_i s_j \rangle \ , \tag{2}$$

where $\langle \cdot \rangle$ denotes a time average along our dynamics. Kinetic and magnetic part of the Hamiltonian can therefore be treated separately.

As a second point, we observe that the link energy satisfies the Boltzmann distribution $\exp(-\beta E_{ij})$, where the fitted constant $\beta = 1/T$ is naturally the inverse temperature of the system (Fig. 1, left-panel). In general, for the homogeneous system we can write $E_{ij} = 4Jn_{ij} + \xi_{ij}$, where n_{ij} is an integer and ξ_{ij} is a constant depending on the initial conditions; since ξ_{ij} does not have any influence, hereafter we set $\xi_{ij} = 0$. Notice that the factor 4 multiplying Jn_{ij} is due to the fact that the minimal amount of exchanged energy is $4J$ (E_{ij} derives from ΔE^m and, apart from possible borders, in rectangular lattices the coordination number is even).

The equilibrium temperature has been verified to be independent from the initial distribution of energies and from the particular link considered, as expected from an intensive quantity. Averages on the links are possibly used only to accelerate the numerical convergence.

The simplest way to evaluate the temperature from the above distribution is to relate β with the average link-energy, obtaining

$$\langle E \rangle \ = \ \frac{\sum_{n=0}^{\infty} 4Jne^{-4J\beta n}}{\sum_{n=0}^{\infty} e^{-4J\beta n}} = \frac{4J}{e^{4\beta J} - 1} \tag{3}$$

which may be easily inverted to get β:

$$\beta = \frac{1}{4J} \log \left(1 + \frac{4J}{\langle E \rangle} \right). \tag{4}$$

In a subsequent check, we verify that $T = 1/\beta$ given by formula (4) is the temperature even for the magnetic variables of the system. Indeed, Fig. 2 evidences that the average magnetic energy $\langle E^m \rangle$ and its fluctuations $\langle (E^m)^2 \rangle - \langle E^m \rangle^2$ are the same in the microcanonical system at temperature T given by Eq. 4 and in a two-dimensional Ising model in equilibrium at temperature T.

Equivalent results are also obtained introducing thermostats at the boundaries of the microcanonical system (Fig.2). The coupling between system and thermostats is imposed by extracting the link energies at the borders every time-step according to the probability distribution $e^{-4\beta Jn}$. We remark that in presence of such thermostats the

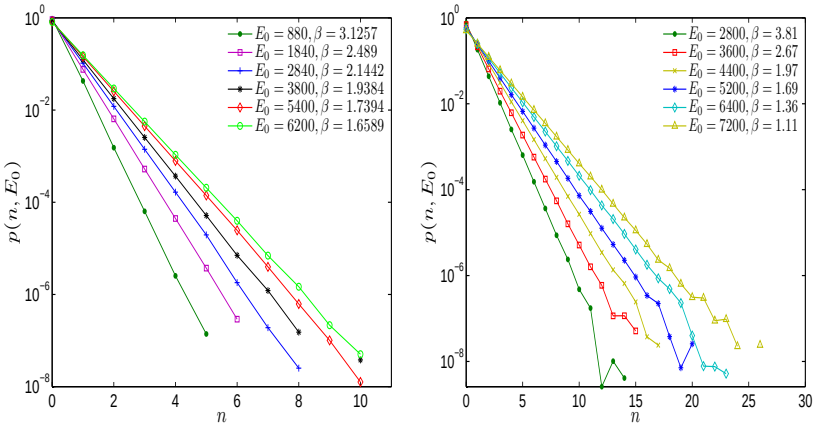


Figure 1. Probability distribution of the kinetic energy per link for an Ising system defined on a square torus of size $L_X = L_Y = 48$ with constant coupling strength J (left panel) and with random J and disorder $\epsilon = 0.2$ (right panel). Results found for different initializations E_0 are reported as shown by the legend. Notice that in the right panel the continuous energy distribution $p(E, E_0), E \in \mathbb{R}$ is approximated by the histogram $p(n, E_0), n \in \mathbb{N}$.

whole system equilibrates at temperature $1/\beta$, independently of the initial conditions, proving the reliability of such a simple model for thermostats.

Energy transport is naturally introduced by imposing different temperatures at the boundaries. Then, whenever a stationary state is reached, Equation (4) provides a simple definition of local temperature. Clearly, along the same column all energies and temperatures are expected to be equal, as they are in fact. The consistency of this definition of local non-equilibrium temperature has been further verified by showing that, at the same T, the local magnetic energy for a link is the same at equilibrium or in the presence of transport (Fig. 2).

In conclusion, the homogeneous system follows a quasi equilibrium picture consistent with the results given by the KQ dynamics [9]. The remarkable difference is that, in the present case, the existence of a local kinetic energy allows a natural definition of temperature, without any reference to the equilibrium magnetic model.

4. From Homogeneous to Disorderd Lattices

After testing our dynamics for the Ising model on a regular lattice with homogeneous coupling, we exploit the fact that, as anticipated, this dynamics is naturally defined even in more complex situations, e.g. when the underlying topology or the interaction couplings J_{ij} are not homogeneous. Here in particular we focus on the case of a 2-dimensional rectangular lattice where the coupling J_{ij} are randomly chosen from a uniform distribution in an interval, i.e. $J_{ij} \in [1-\epsilon, 1+\epsilon]$, $0 < \epsilon < 1$; hence, ϵ is an index of disorder, being the average magnetic interaction fixed and equal to 1.

First of all, we study the differences at equilibrium between homogeneous and disordered systems. To this purpose, using the standard Metropolis dynamics, we evaluate the critical temperature T_C by means of Binder cumulant techniques [18]. Figure (3) shows the value of the critical temperature as a function of the disorder ϵ.

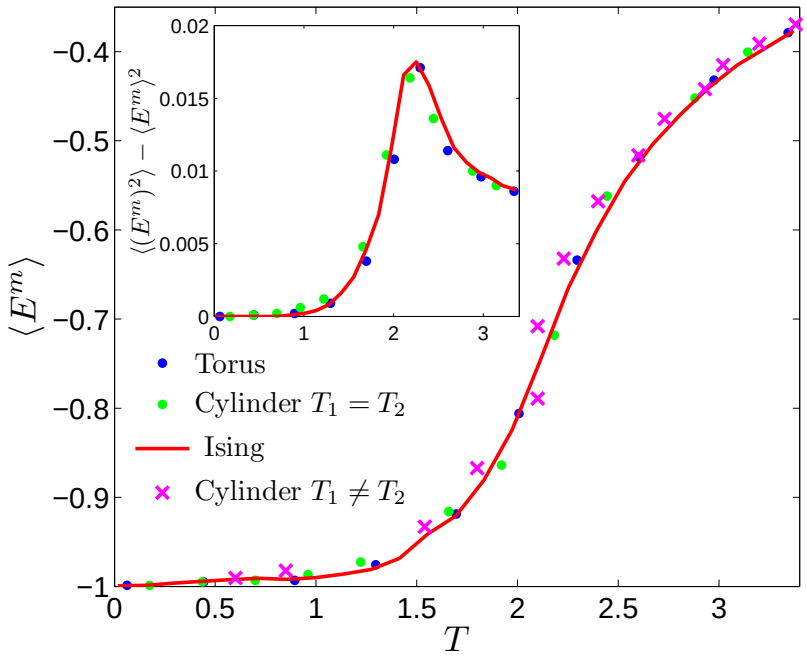


Figure 2. Average magnetic energy per spin $\langle E^m \rangle$ (main figure) and its fluctuations $\langle (E^m)^2 \rangle - \langle E^m \rangle^2$ (inset) as a function of the temperature T for Ising systems of size $N = 2304$ defined on a torus and analyzed with the Metropolis canonical dynamics (continuous line) and with the microcanonical dynamics introduced here (dark •); the case of an Ising system defined on a cylinder endowed with two thermostats set at the same temperature (bright •) or at different temperatures (×) is also considered. The consistency among all cases is clear.

We note that T_C is slightly lowered by the presence of disorder.

Let us now consider the new dynamics for the disordered system. With respect to the homogeneous case $J_{ij} = 1$, the main difference is that the link energy is not of the form $E_{ij} = 4n_{ij}$ with n_{ij} integer. Indeed, the kinetic energy on the link $i \sim j$ can be written as $E_{ij} = \sum'_{k\sim h} J_{kh} n_{kh}$, where $E_{ij} \geq 0$, n_{kh} are integers and the sum $\sum'_{k\sim h}$ runs over $i \sim j$ and its six neighbouring links. Hence, in the sum there are seven different real numbers J_{hk} randomly chosen in $[1-\epsilon, 1+\epsilon]$ and, if all the combinations of integers n_{kh} are realized in the dynamical evolution, the values of E_{ij} can be considered densely distributed along the positive real axis (see Appendix).

Therefore, under the hypothesis of ergodicity we expect that the probability density for link energies is $\exp(-\beta E)$, with E a real number. In Figure (1) we check indeed that in a random system the link energies are distributed according to a continuous exponential function. Also in this case, as in (3), the temperature can be related to the average kinetic energy, in particular for a continuous variable we have

$$\langle E \rangle = \frac{\int_0^\infty z\, e^{-\beta z}\, dz}{\int_0^\infty e^{-\beta z}\, dz} = \frac{1}{\beta}. \tag{5}$$

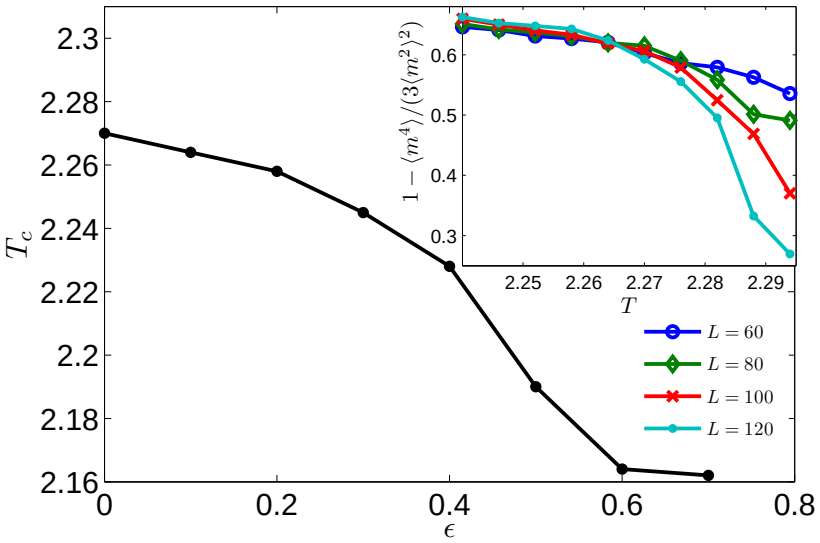


Figure 3. Measure of the critical temperature T_c for systems characterized by different disorder ϵ. The estimate of the critical temperatures has been accomplished by means of Binder cumulants as shown in the inset for the case $\epsilon = 0.1$.

Once again, the constant $1/\beta$ is the temperature T and the link (kinetic) energy equals the system temperature. We check that, although the system is inhomogeneous, the temperature is the same for all the sites, as expected at equilibrium, and also that $\langle E\rangle$ is a consistent definition of temperature even for the magnetic system, as analogously verified for the homogeneous system (see Fig. 2). Therefore, the temperature is the parameter governing the equilibration of the system. In particular, at equilibrium different parts of an inhomogeneous system may display different behaviours but T is constant in the whole sample. For example, if a part of the system is characterized by constant coupling $J_{ij} = J$ while in the rest J_{ij} is chosen randomly, the local kinetic energy is described by discrete and continuous distributions in the different regions respectively. However, the temperature is the same in both. Analogously in a free cylinder (isolated borders) with constant coupling J, we have that the border sites exchange energy with an odd number of neighbours. The minimal amount of exchanged energy is therefore $2J$ instead of $4J$, giving a different discrete distribution for sites in the bulk and at the border. However, we have numerically verified that the temperature does not change.

Thus, in general, for systems with random-incommensurate couplings, Equation (5) provides a good definition of temperature. This definition can naturally be extended to the case when different temperatures are imposed at the boundary thermostats, i.e. in the presence of gradients ($T_2 - T_1 > 0$) and heat transport, as described in the next Section.

5. Transport, Conductivity, Diffusivity

As previously explained, our system satisfies the Boltzmann distribution $\exp(-E/T)$, so that in order to fix a temperature $\bar{T}$ on a given set of links, it is sufficient to extract the relevant link energies according to the distribution $\exp(-E/\bar{T})$, and this is sufficient to establish a consistent coupling between the system and the thermostats. In the following we consider a cylindrical Ising system with boundaries coupled to two thermostats at temperatures T_1 and T_2, respectively, and we study the transport properties. First of all, we verify that in the steady state the kinetic energy $\langle E_{ij} \rangle$ is still well defined on each link. However, in such a non-equilibrium situation, it varies from link to link; hence, hereafter we use $\langle E_{ij} \rangle$ as a definition of *local* temperature T_{ij}. We also notice that once the distance from the thermostats is fixed, its spatial fluctuations increases with ϵ. Hence, the dependence displayed by T_{ij} on the magnetic coupling J_{ij} is very small for ϵ not too large. Now, in the presence of temperature fluctuations also transport is expected to display non trivial spatial patterns arising from the interplay between non-equilibrium and disorder. As a first step in studying such a complex phenomenology we investigate how disorder affects the average transport properties. In particular we introduce the column temperature T_j and magnetic energy E^m_j obtained by spatially averaging over all i's T_{ij} and $\langle E^m_{ij} \rangle$, respectively. The emerging cylindrical symmetry makes j the only gradient variable, and in this situation the simplest model for heat transport is provided by the one-dimensional Fourier equation, where, as usual, the column index j will be treated as a continuous variable x:

$$\frac{\partial E^{tot}}{\partial t} = \frac{\partial}{\partial x}\left(\kappa \frac{\partial T}{\partial x}\right). \tag{6}$$

Notice that E^{tot} is the specific total energy in column j, namely $E^{tot}_j = T_j + E^m_j$, and that κ is the conductivity which is expected to depend only on the local temperature and on the system parameters (J and ϵ in this case). Indeed, in the following we verify that energy transport can be studied by means of equation (6), and we also evaluate κ as a function of T, evidencing the effect of disorder.

In the stationary state, when $\partial E^{tot}/\partial t = 0$, we call Q the total amount of heat crossing any given surface, so that $\partial Q/\partial t$ represents the heat flux which can be measured, for instance, from the energy absorbed per unit of time by the thermostat. As shown in [8], we have

$$\kappa = \frac{\partial Q/\partial t}{\partial T/\partial x}; \tag{7}$$

clearly κ represents the proportionality constant between the temperature gradient and the flowing heat energy. Similarly, the diffusivity of the magnetic energy can be defined as:

$$D = \frac{\partial Q/\partial t}{\partial E^m/\partial x}. \tag{8}$$

It is worth underlining that while D can be obtained directly from the magnetic energy E^m (see Eq. 8) for the conductivity κ we need a measure of the temperature T (see Eq. 7). For this reason KQ dynamics, dealing exclusively with the magnetic energy, allows for the computation of diffusivity, while here we are able to easily estimate both quantities.

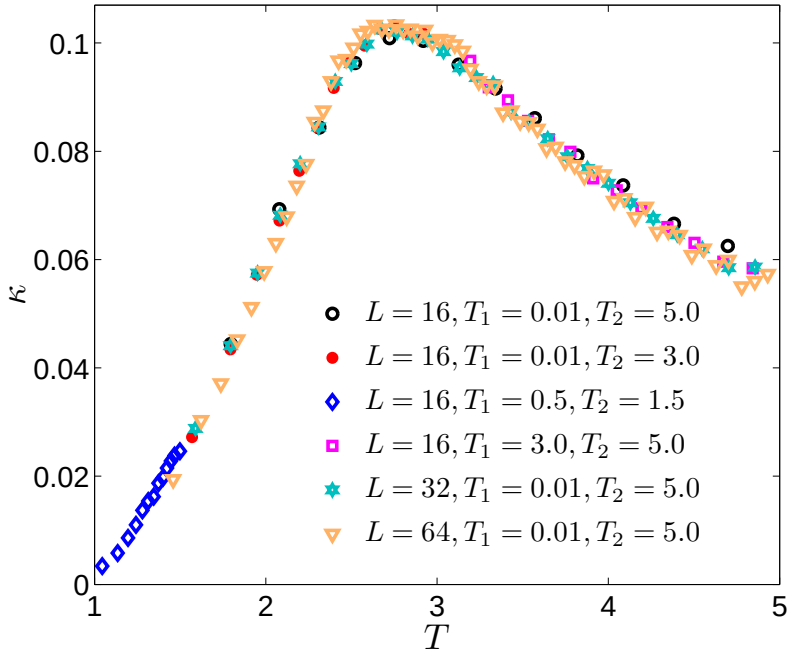


Figure 4. Conductivity versus temperature for an ordered (constant J) Ising system. Different sizes L and different temperature gaps ΔT are considered, as shown in the legend.

Introducing the magnetic specific heat $C = \partial E^m / \partial T$, a comparison of Eq. 7 and Eq. 8 provides the simple relation

$$D = \frac{\kappa}{C}. \tag{9}$$

Notice that C is an equilibrium quantity well known for the Ising model.

We have measured conductivity for the ordered system with $\epsilon = 0$ (Fig. 4) as well as for the disordered system with fixed $\epsilon \neq 0$ (Fig. 5). In both cases we found a very good collapse of data pertaining to different temperatures intervals and sizes.

This provides a strong confirmation of the picture above based on a Fourier transport equation with a temperature (energy) dependent conductivity (diffusivity). In particular, we notice that the curve for the conductivity exhibits a maximum at a temperature $\tilde{T}$ slightly larger than the critical temperature T_C which corresponds to a peak in the specific heat and to a minimum for the diffusivity (see Fig. 6). As observed also in [9], we expect that in the thermodynamic limit the diffusivity goes to zero logarithmically, consistently with the logarithmic divergence of the specific heat, so that the conductivity is not expected to diverge at the critical point T_C. Interestingly, from both Fig. 4 and Fig. 5, we notice that as the temperature is increased, the rate of growth (for $T < \tilde{T}$) and of decrease (for $T > \tilde{T}$) displayed by the conductivity are sensitively different. This point can be understood by looking at Fig. 6 and recalling Eq. 9: at small temperatures the diffusivity remains finite, while the specific heat is close to zero.

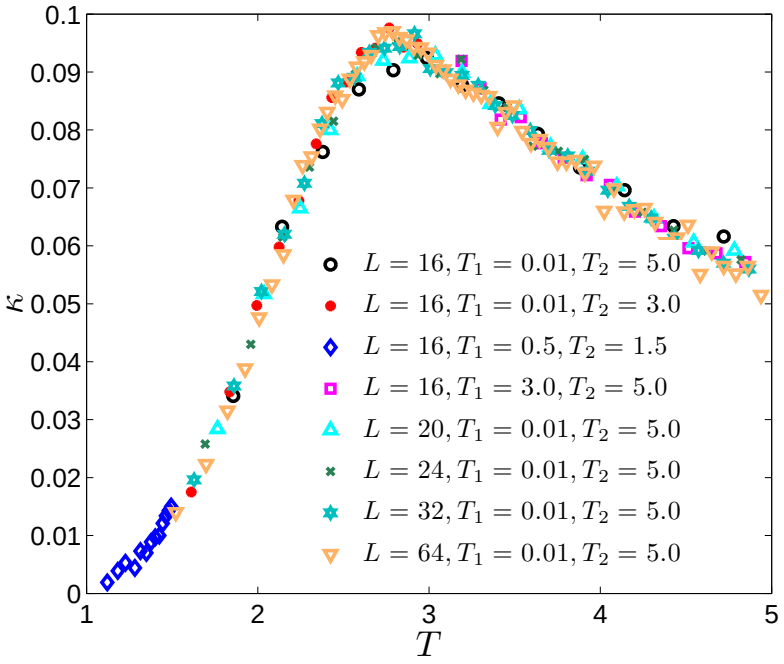


Figure 5. Conductivity versus temperature for a disordered ($\epsilon = 0.2$) Ising system. Different sizes L and different temperature gaps ΔT are considered, as shown in the legend.

6. Effects of Disorder

Let us now deepen our knowledge of how the conductivity is affected by disorder ϵ. In Fig. 7 we show data for conductivity vs. temperature for different degrees of disorder. Remarkably, the figure highlights a clear drift: as the disorder ϵ increases the conductivity κ gets lower for any value of the local temperature. Hence, for a given system characterized by the set of parameters (L_X, L_Y, T_1, T_2) the heat flow $Q(\epsilon)$ is monotonically decreasing with ϵ, or, otherwise stated, the presence of disorder lowers the transport efficiency. We now focus on the behaviour for $\epsilon \to 0$. The transition from the ordered to the disordered case is in fact characterized by different expressions of the kinetic energy as a function of the temperature (see Eqs. 4, 5). This could be a signal of a non trivial behaviour also for different physical quantities. A plausible ansatz for a singularity at sufficiently small ϵ is provided by the expansion:

$$Q(\epsilon) \sim Q(0) - A\epsilon^{\alpha}, \tag{10}$$

where $A > 0$ is expected to depend in general on the system parameters (size, gradient $T_2 - T_1$, etc) and α is a possibly universal exponent. In Fig. 8 we show a log-log scale plot for $Q(0) - Q(\epsilon)$ which confirms the scaling law of Eq. 10 over a wide range of disorder and for different choices of temperature intervals.

By means of a fitting procedure it is possible to get estimates for A and α. Interestingly, A increases with the temperature gap $T_2 - T_1$, and its value is significantly smaller when both temperatures are larger than the critical one, namely $T_2, T_1 > T_C$.

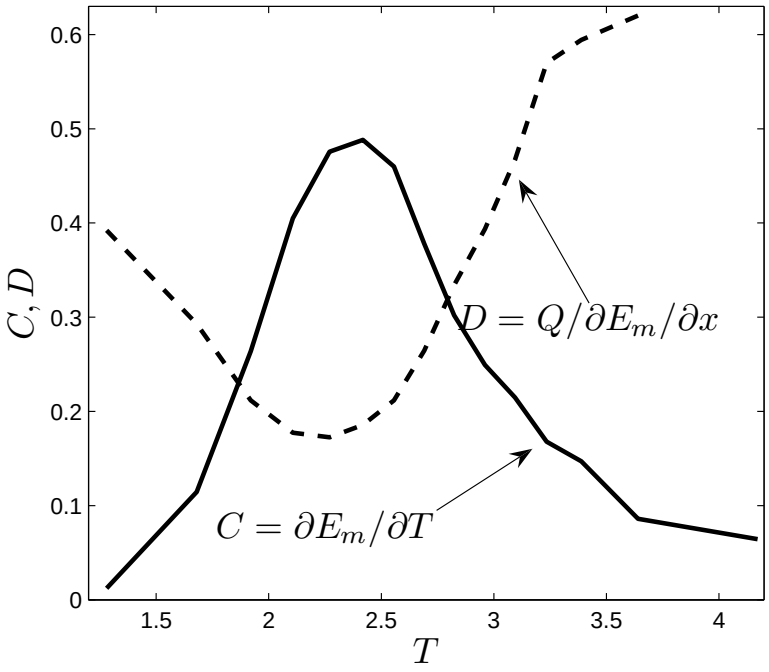


Figure 6. Specific heat C (continuous line) and diffusivity D (dashed line) as a function of the temperature T, for an ordered Ising system ($\epsilon = 0$) of size $L = 16$ and thermostats at temperatures $T_1 = 0.01, T_2 = 5.0$.

Hence, as expected, the effect of disorder is especially appreciable for low temperatures. We also notice that, within the error, the agreement among the exponents α is rather good.

Finally, we remark that when $\epsilon \ll 1$ and both T_1 and T_2 are smaller than T_C the decorrelation time are long and the measures of $Q(\epsilon)$ and α, the relevant exponent, get awkward. Indeed, the "critical slowing down" observed for $\epsilon \to 0$ is neatly distinct from the behaviour at $J = 1$ (i.e. $\epsilon = 0$). This provides a hint on a possible non analiticity as $\epsilon \to 0$.

7. Conclusions

We have introduced a microcanonical dynamics based on the link reserves of kinetic energy, showing that it recovers the results on regular lattices previously obtained by other dynamics and that, moreover, it can be properly applied to disordered systems and it lets a natural definition of temperature, also when far from equilibrium. This allows an easy access to such quantities as conductivity and specific heat, otherwise difficult to define operationally. We measured the average conductivity for the ordered and the disordered systems showing that the presence of disorder reveals in the reduction of the transport efficiency.

The disordered lattice exhibits remarkable additional features: there are indications for a singular behaviour of the system in the limit $\epsilon \to 0$ of the disorder

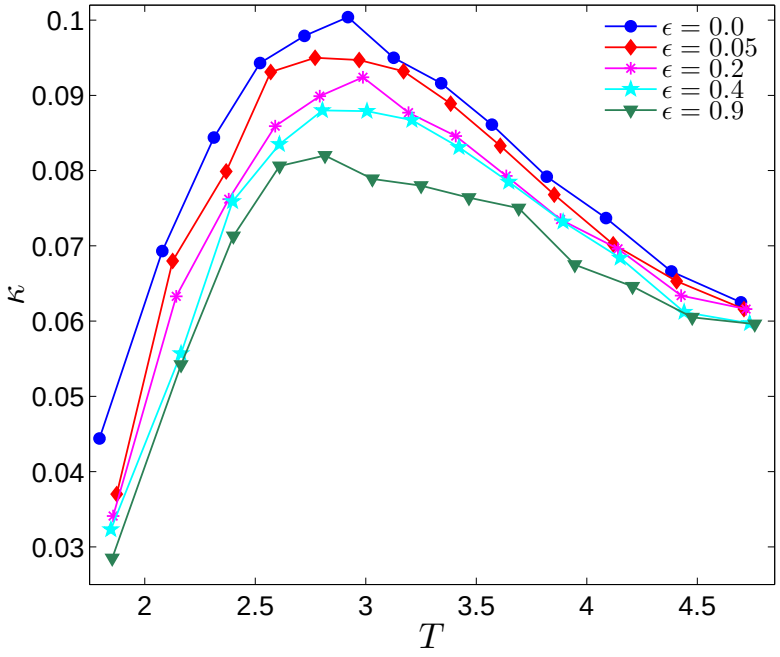


Figure 7. Conductivity versus temperature for a disordered Ising system of size $L = 16$ and fixed temperature gap $T_1 = 0.01, T_2 = 5.0$. Different values of disorder ϵ are considered, as shown in the legend.

parameter. The reason of such a singularity may lie in the numerical strain in filling the reals by combinations with integer coefficients if the couplings J_{ij} are very close to each other. This slowing down should be the dynamical counterpart of the discontinuity of the temperature (see expressions (3) and (5)) when the 2ϵ-width of the disorder interval tends to zero. Moreover, it would be interesting to highlight the nature of the exponent α, which describes how the heat flow decreases with ϵ. In particular, it should be clarified whether α depends on the system parameters (L_X, L_Y, T_1, T_2) or, if not, whether it depends on the particular dynamics chosen.

Recalling from past experiments that the sole presence of gradients proved influent on the fluctuations of physical and geometrical observables [9], on the basis of present results it seems likely that there are other problems deserving future investigations, e.g. the fine interplay between disorder and non-equilibrium in small scale regions, where local heat flows and temperature fluctuations interact presumably in non trivial ways. In other words, for the disordered system we have verified the effectiveness of the Fourier approach by considering averaged quantities, while the validity of such a description at the microscopic scale is still an open problem.

Finally, we underline that the dynamics introduced here allows possible extensions not only to varied types of disorder (vacancies, negative couplings, dynamical disorder...) or to spin systems lying on different geometrical structures, but also to systems where the gradient maintaining the condition of non-equilibrium is due, for instance, to the contact with reservoirs at different densities [19]. In general, it is

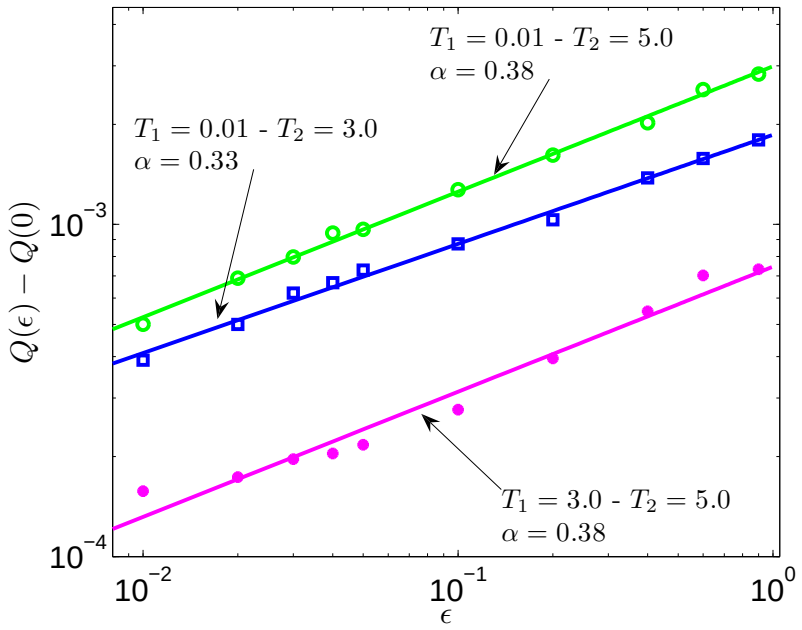


Figure 8. Loglog-scale plot for $Q(0) - Q(\epsilon)$ versus ϵ. Different symbols refer to different temperature gaps, while the continuous line represent the best linear fit. The error on the exponent α is approximately 10%.

conceivable to model some peculiar dynamics where "conservation" refers to the sum of two distinct populations.

Appendix A.

Let $\theta_1, ..., \theta_m$, with $m \geq 2$, positive and rationally independent reals. Let $X > 0$. Then, for arbitrarily small δ, there exists a linear combination with integer coefficients

$$C = \sum_{k=1}^{m} N_k \theta_k$$

such that $0 \leq \mid X - C \mid < \delta$.
Proof : let λ_0 and M_0 be the minimal and the maximal positive reals obtained as integer combinations $\sum_{k=1}^{m} u_k \theta_k$, where u_k may be $1, 0, -1$. Then define a_0 as the greatest positive real $0 < a_0 < \lambda_0$ of the form

$$a_0 = M_0 - k_0 \lambda_0,$$

with integer k_0. Such a number a_0 is an integer combination of the $\{\theta_k\}$ and it does not coincide with λ_0 because of their rational independence. We define now

$$\lambda_1 = \min\{a_0, \lambda_0 - a_0\},$$

observing that necessarily $\lambda_1 < \lambda_0/2$.

Now, we iterate the procedure defining

$$a_n = M_0 - k_n \lambda_n,$$

and

$$\lambda_{n+1} = \min\{a_n, \lambda_n - a_n\}.$$

We obtain a positive sequence λ_n converging to 0, because $\lambda_{n+1} < \lambda_n/2$. Each term in this sequence is an integer combination of the $\{\theta_k\}$. Now, we can choose N in such a way that $\lambda_N < \delta$. Since λ_N is finite, there exists an integer p such that

$$p\ \lambda_N < X < (p+1)\ \lambda_N.$$

We get this way a neighborhood of X smaller than δ, whose extremes are integer combinations of the $\{\theta_k\}$, QED.

Note 1: the way X has been approximated does not necessarily correspond to an optimal strategy;
Note 2: with reference to our problem, where the $\{\theta_k\}$ are the seven couplings J_{ij} chosen for each link in an interval $[1-\epsilon, 1+\epsilon]$, and the integer coefficients are the iterated additions and subtractions determined by the wandering spin flips, it seems that, especially for great X's, the probability of the right approximating combination is extremely low. However, in the integrals of formula (5), the real variable is weighted in turn by the Boltzmann factor, and this explains why also in our finite-time simulations it is possible to to fill densely the relevant part of the real axis, ensuring the correctness of the procedure;
Note 3: when the 2ϵ-width of the interval shrinks (little disorder), this contributes to make difficult the approximation: the reduction in numerical efficiency in these conditions may be observed indeed, as noticed in Section (6), and it could also be related to the possible singularity of the limit $\epsilon \to 0$.

[1] Lepri S, Livi R and Politi A, 2003 *Phys. Rep.* **377**, 1
[2] Deutsch JM and Berger A, 2008 *Phys. Rev. B* **77**, 354
[3] Gaspard P and Gilbert T, 2008 *New J. Phys.* **10**, 103004
[4] Baldovin F, Chavanis P-H and Orlandini E, 2009 *Phys. Rev. E* **79**, 011102
[5] Vichniac GY, 1984 *Physica* **10D**, 96
[6] Pomeau Y and Vichniac GV, 1988 *J. Phys. A: Math. Gen.* **21**, 3297
[7] Toffoli T and Margolus N, *Cellular Automata Machines: A New Environment for Modeling* (The MIT Press, Cambridge 1987) 185-205
[8] Casartelli M, Macellari N and Vezzani A, 2007 *Eur. Phys. J. B* **56**, 149
[9] Agliari E, Casartelli M and Vezzani A, 2007 *Eur. Phys. J. B* **60**, 499
[10] Hinrichsen H, 2008 *J. Stat. Mech.* P02016
[11] de Queiroz SLA and Stinchcombe RB, 2008 *Phys. Rev. E* **78**, 031106
[12] Dhar A and Saito K, 2008 *Phys. Rev. E* **78**, 061136
[13] Karahalios A, Metavitsiadis A, Zotos X, Gorczyca A and Prelovšek P, 2009 *Phys. Rev. B* **79**, 024425
[14] Ben-Naim E and Krapivsky PL, 2009 *Phys. Rev. Lett.* **102**, 190602
[15] Harris R and Grant M, 1988 *Phys. Rev. B* **38**, 9323
[16] Saito K, Takesue S and Miyashita S, 1999 *Phys. Rev. E* **59**, 2783
[17] Neek-Amal M, Moussavi R and Sepangi HR, 2006 *Physica A* **371**, 424
[18] Binder K, 1997 *Rep. Prog. Phys.* **60**, 487
[19] Agliari E, Casartelli M and Vezzani A, 2008 *Eur. Phys. J. B* **65**, 257